

# BEMD based adaptive Lee filter for despeckling of SAR images

Ranjith Kumar Painam<sup>a</sup>, Suchetha Manikandan<sup>b,\*</sup>

<sup>a</sup> School of Electronics Engineering, Centre for Healthcare Advancement, Innovation and Research, VIT University, Chennai, Tamil Nadu 600127, India

<sup>b</sup> Centre for Healthcare Advancement, Innovation and Research, School of Electronics Engineering, VIT University, Chennai, Tamil Nadu 600127, India

Received 4 April 2022; received in revised form 25 November 2022; accepted 3 December 2022

Available online 20 December 2022

## Abstract

Synthetic aperture radar (SAR) image processing finds application in gathering features to detect the ecological changes in earth observatory. But the speckle noise in the acquired image degrades the quality of detection. This paper explains a new method to minimize speckle noise in SAR images using bidimensional empirical mode decomposition (BEMD) based adaptive Lee filter. The main innovation of this proposed work is the use of the BEMD technique on SAR images. The decomposed levels are called bidimensional intrinsic mode functions (BIMF). By this decomposition algorithm, the high-frequency noise component gets separated in the first level of BIMF, which is further filtered by the proposed adaptive filter and reconstructed. In this paper, we are proposing a BEMD based adaptive Lee filter. The BEMD based Lee filter with different window sizes is used. The designed filter algorithm is validated by calculating the performance parameters to demonstrate its denoising performance.

© 2022 COSPAR. Published by Elsevier B.V. All rights reserved.

**Keywords:** Adaptive filters; BEMD; Synthetic aperture radar image processing; Speckle noise; Image reconstruction

## 1. Introduction

Synthetic Aperture Radar (SAR) is an emerging area of research (Jayanthi Sree and Vasanthanayaki, 2019). Synthetic Aperture Radar (SAR) is an emerging research area in the field of remote sensing. The SAR technique is used to obtain two-dimensional high-resolution images in all weather conditions (Liu et al., 2016; Baraldi and Parmiggiani, 1995; Elgamel and Soraghan, 2011; Xu et al., 2016; Kabir and Bhuiyan, 2015). The major applications of SAR includes for monitoring and mapping vegetation, land cover, land-use change, sea oil slick pollution monitoring, military, geology and agriculture (Bhuiyan et al., 2009; Bhuiyan et al., 2010; Devapal et al., 2019). Automatic processing of the SAR images was extremely difficult because of the presence of speckle noise (Gao et al., 2006). The existence of speckle noise in the SAR

images collection is one of the main drawbacks and is quite challenging for remote sensing applications (Jian et al., 2012; Jiang and He, 2017; Kittisuwan, 2018). The speckle noise in the SAR image is mathematically modelled as a multiplicative noise, which corrupts the original information in the image and very difficult to process it (Kumar et al., 2017; Linderhed, 2009). This is occurred due to the constructive and destructive interference of multiple back-scattered echo signals, and consequently degrades the resolution of the acquired SAR images. Therefore, the suppression of speckle noise has great impact in digital image processing (Lu et al., 2017). Speckle noise filtering is a vital step in the pre-processing of SAR data (Myakinin et al., 2013). This is a multiplicative noise that causes many issues during the processing of images in applications related to remote sensing (Nunes and Deléchelle, 2009). In recent years, there are lots of researches happening in speckle noise reduction techniques that underlies reflectivity and scattering properties of the targets (Passoni et al., 2004; Sreelatha and Ezhilarasi, 2019). The speckle noise fil-

\* Corresponding author.

E-mail address: [suchetha.m@vit.ac.in](mailto:suchetha.m@vit.ac.in) (S. Manikandan).

tering techniques have two main goals, one is, removing the noise of the speckle and the other is preserving the details in a SAR image. Several approaches have been developed over the last two or three decades to nullify the speckle noise in SAR images (Sumaiya and Kumari, 2017). Traditional SAR image denoising methods are typically categorised into two techniques: one is spatial domain technique which deals with the noisy filter image, and the second one is transform domain technique which uses a filter with a different function (Dorini and Leite, 2013).

### 1.1. Related works

There are several adaptive speckle filters that helps to manage image speckling. To minimize the speckle noise in SAR image, a minimum mean squared error (MMSE) filter in the non-sub sampled contourlet transform domain is adopted (Jiang and He, 2017). The despeckling goal is to effectively reduce the speckle from SAR images while preserving the image valuable information. A stokes-based sigma filter is used in homogeneous regions that eliminate speckle noise and also retains information in heterogeneous regions. This filter has the potential to maintain a strong target point (Sreelatha and Ezhilarasi, 2019). A Nonlocal means (NLM) filter is popularly used for speckle filtering and preserving subtle information, but still has a few shortcomings. The disadvantage of the NLM filter is its biased estimation due to excessive speckle noise. In recent works, the measure of similarity that preserves polarimetric data or scattering property is also the area of interest. A technique of speckle-noise filtering is given which retains the polarimetric properties and fine SAR polarimetric data structures. This results in an objective estimation of excessive noise. This filtering approach adjusts weights iteratively to minimize the distance (Sumaiya and Kumari, 2017). A shift-invariant K-means singular value decomposition (K-SVD) and the guided filter is used for denoising of the SAR image. This is a multistep method. The first step deals with the noisy image with the K-SVD shift-invariant and the initial de-noised image is obtained. The guided filtering is used for the initial denoised image in the second step. The final denoised image shows that this process not only has better visual effects and unbiased assessment but when denoising SAR images it can also save more detailed information such as image edge and texture (Dorini and Leite, 2013). Speckle noise is considered as a multiplicative noise in a SAR image. Xu. et al. discussed the fields of expert technique, used a Markov random field model based on a higher-order filter for reducing speckle noise (Xu et al., 2019). Effective feature extraction and elimination of the nearest neighbour distance interference matching method is addressed and a conventional scale-invariant feature transform (SIFT) algorithm were used to describe local features (Yang et al., 2017). A Dual-tree complex wavelet transform (DTCWT) method is used to minimize the speckle variations in the intensity of SAR image (Lee, 1980). To despeckle and extract geographical

features in SAR image wavelet-based speckle filtering is used. This is developed based on multiscale image analysis. In the wavelet domain-based filtering approach, the main concept is to transform multiplicative noise into additive noise. Speckle noise is reduced by increasing the pixel amplitude with respect to diagonal, vertical, and horizontal axis. Therefore, there is always a trade-off between speckle reduction and detail preservation (Lopes et al., 1990). Up to now, many filtering methods are employed to suppress speckle noise from SAR images. Some filters are good for visual interpretation, while others are good for smoothing and noise reduction capabilities. Enhanced Frost, Mean, Kuan, Median, Frost, Lee, Wiener, and Gamma MAP filters are some examples of such filters. Some of these use window techniques to suppress speckle noise called a kernel. This window size may vary from 3X3 to 7X7 and it has to be odd. To achieve better results, the window size should be smaller. A method is presented in which each pixel is given a window depending on the size of the object in the image. SAR images are filtered by applying optimal windows to the real in-phase and imaginary quadrature components, with separate windows applied to the pixels of the intensity image. Both the single-polarized and multi-polarized SAR images are provided in the demonstration of the suggested methodology (Mahdavi et al., 2018). In the literature (Liu et al., 2016; Baraldi and Parmiggiani, 1995; Elgamel and Soraghan, 2011; Xu et al., 2016; Kabir and Bhuiyan, 2015), various filtering methods are implemented to reduce the noise variations in SAR images. In the present work, we proposed a filtering technique in the spatial domain with various levels of speckle-noise components. The major contributions of this work are summarised as follows. i) The BEMD methodology is applied to the SAR image database, which is collected from Sandia National Laboratory. ii) The proposed BEMD based adaptive Lee filter uses three BIMF levels. iii) The first BIMF level is obtained after performing BEMD decomposition on the input image is adaptively filtered. iv) Calculating performance metric values. v) The proposed filter that uses three different window sizes.

### 1.2. Formation of speckle noise in SAR images

The speckle corrupted of an obtained SAR image is formulated as follows:

$$P(k, l) = Q(k, l).R_n(k, l) \quad (1)$$

where  $(k, l)$  indicates the degraded pixel of the obtained SAR image,  $Q(k, l)$  represents the noise free image to be reconstructed, and  $R(k, l)$  denotes the unwanted speckle noise over the parameters of unit variance and mean.

## 2. Theoretical background

In the last few decades, the BEMD has been commonly used as a potential tool for processing the images. Compared to existing methods like Fourier analysis and wavelet

transform, the BEMD is quantitative, adaptive and intuitive. The decomposition is designed to extract the BIMF adaptively from the given image with different oscillations. Nunes et al. initially extended the EMD to the scenario of 2-D data. They used a radial basis function (RBF) to get envelopes to test the local properties of the BEMD and replaced the Hilbert transformation with Riesz transform (Jiang and He, 2017; Kittisuwan, 2018; Kumar et al., 2017). Linderhed et al. consider interpolation of the triangle based cubic spline as well as interpolation of the thin-plate spline (Lu et al., 2017).

### 2.1. BEMD algorithm

Here, we consider an SAR image with speckle noise as an input image and compute upper and lower envelopes. The flow chart of the BEMD decomposition process is shown in Fig. 1. Next step is to calculate the mean for every spatial position and subtracting the mean envelope from the input image. This entire process is called as sifting. Here we have to follow two conditions. First one is, when envelope mean is close to zero then we will get first BIMF SAR image otherwise continue the above process till getting the first BIMF SAR image. This iteration process is proceeded till a residue image is obtained.

### 2.2. Adaptive filters

Many different methods are used to eliminate speckle noise based on the phenomenon of various mathematical models. Adaptive speckle filtering is more useful in texture areas and it is best to retain edge details. An adaptive Lee filter is a filter that has self-adjusting characteristics. It is capable of adjusting its filter coefficients automatically to adapt the input signal via an adaptive algorithm. We have used the term adaptive filter in the paper to indicate the adaptability of the filter in selecting the window size and filter coefficients based on the image. The detailed develop-

ment and implementation of the proposed BEMD based adaptive Lee filter are discussed in the succeeding sessions.

## 3. Proposed technique

In the proposed filtering approach, the input speckle-noise image is decomposed into different levels of BIMF. This approach mainly depends on the following two conditions. Firstly, each decomposition level in the BIMF should maintain a number of zero crossings and extrema. Secondly, concerning the local mean of each BIMF must be symmetric. Fig. 2 illustrates the proposed adaptive filtering process using the BEMD technique. After decomposition using BEMD, the first level of BIMF is adaptively filtered using the designed adaptive filters. Further, the filtered BIMF image is added with the remaining BIMFs of BEMD decomposition to get despeckled SAR image. The designed adaptive filter is explained in the forthcoming sessions.

### 3.1. BEMD based adaptive Lee filter

The proposed BEMD based Lee filter uses the local statistics to retain the details and finds its application in the multiplicative speckle model (Yang et al., 2017). This adaptive filter performs the smoothing operation for low noise variance compared to the higher variance of the noise. Thus, due to the filter adaptive nature, it can preserve details in low as well as high contrast. The equation for the filtered image is represented by

$$x(i, j) = m_i + W * (P_c - m_i) \quad (2)$$

where  $(i, j)$  represents the pixel value after filtering,  $m_i$  indicates the mean intensity of the filter window,  $P_c$  represents the center of the pixel,  $W$  is the filter window and is defined as

$$W = \sigma^2 / (\sigma^2 + \rho^2) \quad (3)$$

$\sigma$  indicates the pixel variance and it is calculated as

$$\sigma^2 = \frac{1}{T} \sum_{j=0}^{T-1} X_j^2 \quad (4)$$

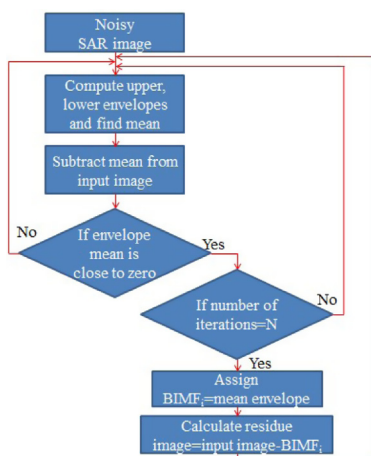


Fig. 1. BEMD decomposition process.

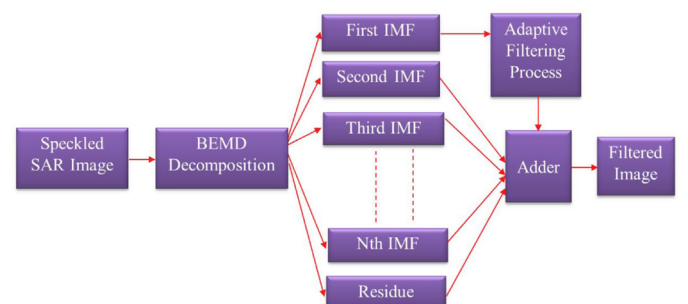


Fig. 2. Proposed BEMD based despeckling of SAR image.

where  $T$  is the filter window size,  $X_j$  denotes the value of the pixel at  $j$ ,  $\rho$  represents the variance of the additive noise. The variance is defined as the  $M$  size of the image

$$\rho^2 = \frac{1}{M} \sum_{j=0}^{M-1} Y_j^2 \quad (5)$$

where  $Y_j$  indicates the value of the pixel at  $j$

### 3.2. Development of BEMD based Lee filter

First, to determine the filter physical form, use the minimum mean square error (MMSE) criterion. Then, assuming that the image data is stationary  $f(x, y)$  is calculated from  $I(x, y)$ . The impulse response  $m(t)$  and the MMSE filter transfer function  $M(r)$  provide an approximation of  $f(x, y)$  from  $I(x, y)$  by nullifying the filter mean square error of the filter  $\epsilon^2$  given by

$$\epsilon^2 = E[(f(t) - I(t) * m(t))^2] \quad (6)$$

the above Eq. (6) is modified with spatial coordinates  $t = (x, y)$ . A transfer function is obtained by MMSE

$$M(r) = \begin{cases} \left[ \frac{\bar{n} S_f(r)}{S_f(r) * S_n(r)} \right] \frac{1}{H^*(r)}, & r \neq 0 \\ \frac{1}{\bar{n}}, & r = 0 \end{cases} \quad (7)$$

where  $\bar{n} = E[n(t)]$  and  $r = (r_x, r_y)$  is the spatial frequency coordinate.  $S_f(r)$  and  $S_n(r)$  are the reflectivity of the power spectral densities and the noise process respectively. In Eq. (7),  $H^*(r)$  represents the complex conjugate of the transfer function of the system that is not data-dependent and can thus be viewed as constant. The remaining part of  $M(r)$  is  $\frac{\bar{n} S_f(r)}{S_f(r) * S_n(r)}$  (denoted as  $M_I(r)$ ) and it can be used as data-dependent. The basic model for  $f(t)$  is an autoregressive system with an autocorrelation function of  $R_f(\tau)$  and an  $S_f(r)$  two-sided power spectral density of the form

$$R_f(\tau) = \sigma_f^2 e^{-a|\tau|} + \bar{f}^2 \quad (8)$$

where the parameters  $\sigma_f^2$ ,  $a$  and  $\bar{f}^2$  have different values for different terrain categories.

$$S_f(r) = \frac{2\sigma_f^2 a}{a^2 + 4\pi^2 r^2} + \bar{f}^2 \delta(r) \quad (9)$$

The correlation  $R_n(\tau)$  and power spectral density  $S_f(r)$  for the multiplicative white noise are

$$R_n(\tau) = \sigma_n^2 \delta(\tau) + \bar{n}^2 \quad (10)$$

$$S_n(r) = \sigma_n^2 + \bar{n}^2 \delta(r) \quad (11)$$

where the parameters  $\sigma_n^2$  is the variance of SAR image and  $\bar{n}^2$  denotes the number of looks. With the  $f(t)$ ,  $n(t)$  and  $M_I(r)$  power spectral densities, we can deduce the filter impulse response as

$$m(t) = K_1 \alpha e^{-\alpha|t|} \quad (12)$$

and

$$\alpha = \sqrt{2a \left[ \frac{\bar{n}}{\sigma_n} \right]^2 \cdot \left[ \frac{1}{1 + \left( \frac{\bar{f}}{\sigma_f} \right)^2} \right]} + a \quad (13)$$

where the decay constant  $\alpha$  depends across all three signal parameters  $\sigma_f$ ,  $a$  and  $\bar{f}$ . The uniform area  $a$  will vary slightly. Thus,  $a$  is used as a constant for filter adaptation. The steps involved in implementation of the BEMD based Lee filter are narrated in the Algorithm 1.

---

Input image: First level of BEMD decomposition

1: Decompose noisy image using BEMD to get

$BIMF_{l,m}(i, j)$

2: Take first  $BIMF_{l,m}(i, j)$

3: Apply BEMD based Lee filter with  $BIMF_{l,m}(i, j)$

4: Apply a window centered around the pixel  $(i, j)$

5: Compute the local mean  $M_L$  and variance  $V_L$  of the filter window

6: Calculate noise mean  $M_N$  and noise variance  $V_N$  of the input image

7: From the above values compute weighting function  $K$

$$K = \frac{M * L_V}{(L_M * L_M * M_V)(M * M * L_V)}$$

where  $M$  is the multiplicative noise mean and  $M_V$  is the multiplicative noise variance,  $L_M, L_V$  is the local mean and variance

Output image: Despeckle image

---

## 4. Performance parameters

In order to evaluate the effectiveness of the proposed filter in speckle noise reduction the following performance parameters were calculated for 2-dimensional SAR image.

### 4.1. Equivalent Number of Looks (ENL)

ENL calculation is performed on the intensity variations of the image to quantify the level of speckle noise. If the ENL value is high then the reconstruction performance is good in suppression of speckle noise otherwise the reconstruction quality will be poor.

$$ENL = \left[ \frac{\mu}{\sigma} \right]^2 \quad (14)$$

where  $\mu$  and  $\sigma$  indicate the mean and standard deviation

### 4.2. Speckle Suppression Index (SSI)

This is the filtered image variance coefficient that is standardized with the original image.



$$SSI = \frac{\sqrt{\text{Var}(I_f)} X \frac{\text{mean}(I_o)}{\sqrt{\text{Var}(I_o)}}}{\text{mean}(I_f)} \quad (15)$$

where  $I_f$  is the filtered image,  $I_o$  is the noisy image. SSI value will be less than one if the filter is more efficient in reducing the noise.

#### 4.3. Structural Similarity Index Measure (SSIM)

SSIM is utilized to find the correlation between the original and reconstructed images. The higher SSIM value means lesser the noise in the filtered image and preserves the original details.

$$SSIM = \frac{(2\mu_p\mu_q + C_1)(2\sigma_{pq} + C_2)}{(\mu_p^2 + \mu_q^2 + C_1)(\sigma_p^2 + \sigma_q^2 + C_2)} \quad (16)$$

where  $p$  and  $q$  denotes the original and filtered SAR images respectively,  $\mu_p$  and  $\mu_q$  is the mean,  $\sigma_{pq}$  represents the covariance of  $p$  and  $q$ ,  $\sigma_p^2$  and  $\sigma_q^2$  is the standard deviation,  $C_1=(a_1L)^2$  and  $C_2=(a_2L)^2$  are the two variables for balancing the division with a lower denominator,  $L$  represents the pixel value range (normally this is 255 for 8-bit grayscale images)  $a_1=0.01$  and  $a_2=0.03$  by default.

## 5. Results and discussion

SAR images used in the proposed work have been collected from Sandia National Laboratory using the following link. <http://www.sandia.gov/radar/complex-data/>. The



Fig. 3. Database SAR image.

original SAR image size is 3000X1754, date of acquiring 2006:03:01 and time of acquiring 14:31:01. The proposed BEMD based adaptive Lee filter algorithm demonstrated using numerical simulations with Matlab version R2021a in Intel core i5-8050, 8 Gb RAM system configuration. After getting different BIMF levels from BEMD decomposition, we select the first BIMF SAR image with speckle noise because the highest frequency component is get separated in first BIMF level. Now, this first BIMF is adaptively filtered. To carry out the simulation study, the speckle noise with a variance of different values are added to the SAR image. Fig. 3 depicts the original input SAR image taken from the database. Fig. 4 shows the BEMD decomposition. Fig. 4(a) illustrates the noisy SAR image with a variance of 0.05. The resultant BEMD-BIMF levels are represented in Fig. 4(b)-(d). Our proposed BEMD based adaptive Lee filter algorithm is elaborated as the Algorithm 1. The performance of the proposed filtering algorithm is evaluated in two distinct ways. (i) reconstruction quality of the visual check, and (ii) calculation of filter performance metrics. Fig. 5(a)-(c) project the reconstructed SAR image using BEMD based Lee filter having speckle variance of 0.01 with 3X3, 5X5 and 7X7 window sizes. Fig. 6(a)-(c) project the reconstructed SAR image using BEMD based Lee filter having speckle variance of 0.05 with different window sizes of 3X3, 5X5 and 7X7. Figs. 7–10 shows the reconstructed SAR images of several conventional filters with different window sizes. From Figs. 3–10 it can be seen that the visual quality of the filtered image looks similar to the original input image. However, the proposed BEMD based adaptive Lee filtering method obtained the best performance for 3X3, 5X5, 7X7 window sizes in terms of quantitative analysis such as SSI, SSIM, and ENL compared to conventional filtering methods. The performance analysis of the proposed filtering approach and conventional methods are tabulated in the Tables. 1–3. If the filter output is effective in reducing the speckle noise, the SSI index tends to be less than 1. Lower values indicate better performance of speckle filtering. We have compared the proposed filter SSI values with conventional filters as shown in Table 1. The proposed filter SSI value is 0.841 for a 3X3 window size, 0.851 for a window

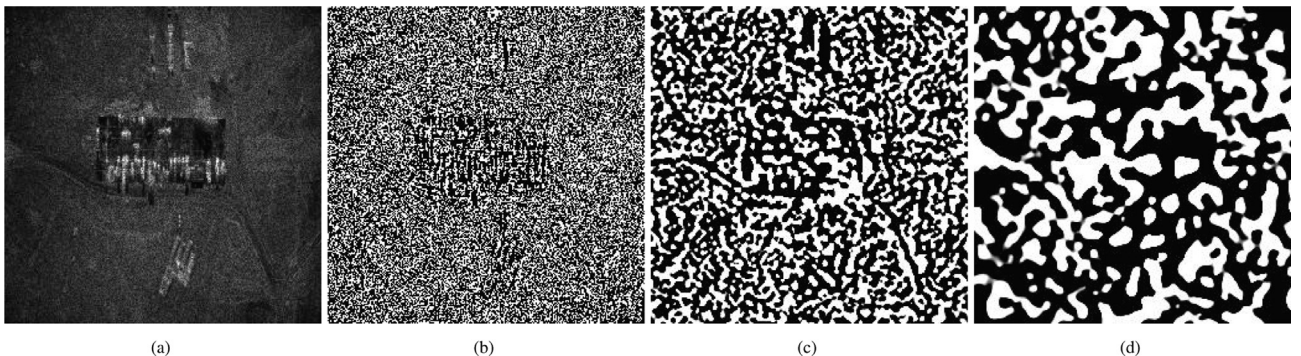


Fig. 4. BEMD decomposition (a) Speckle corrupted SAR image (b) first level of BIMF (c) second level of BIMF (d) third level of BIMF.

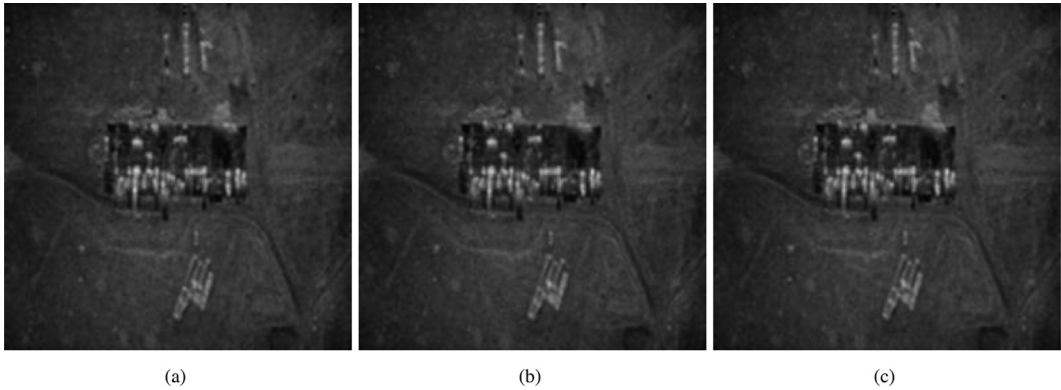


Fig. 5. Reconstructed SAR image using BEMD based Lee filter with speckle variance of 0.01. (a) 3×3 (b) 5×5 (c) 7×7.

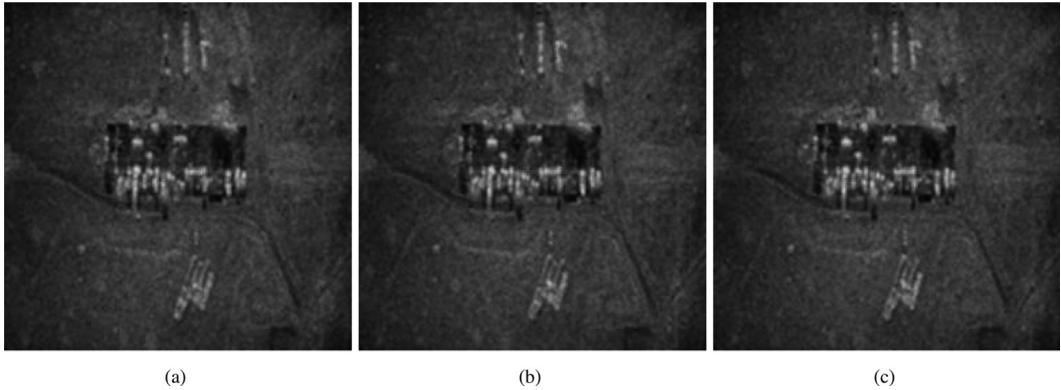


Fig. 6. Reconstructed SAR image using BEMD based Lee filter with speckle variance of 0.05. (a) 3×3 (b) 5×5 (c) 7×7.

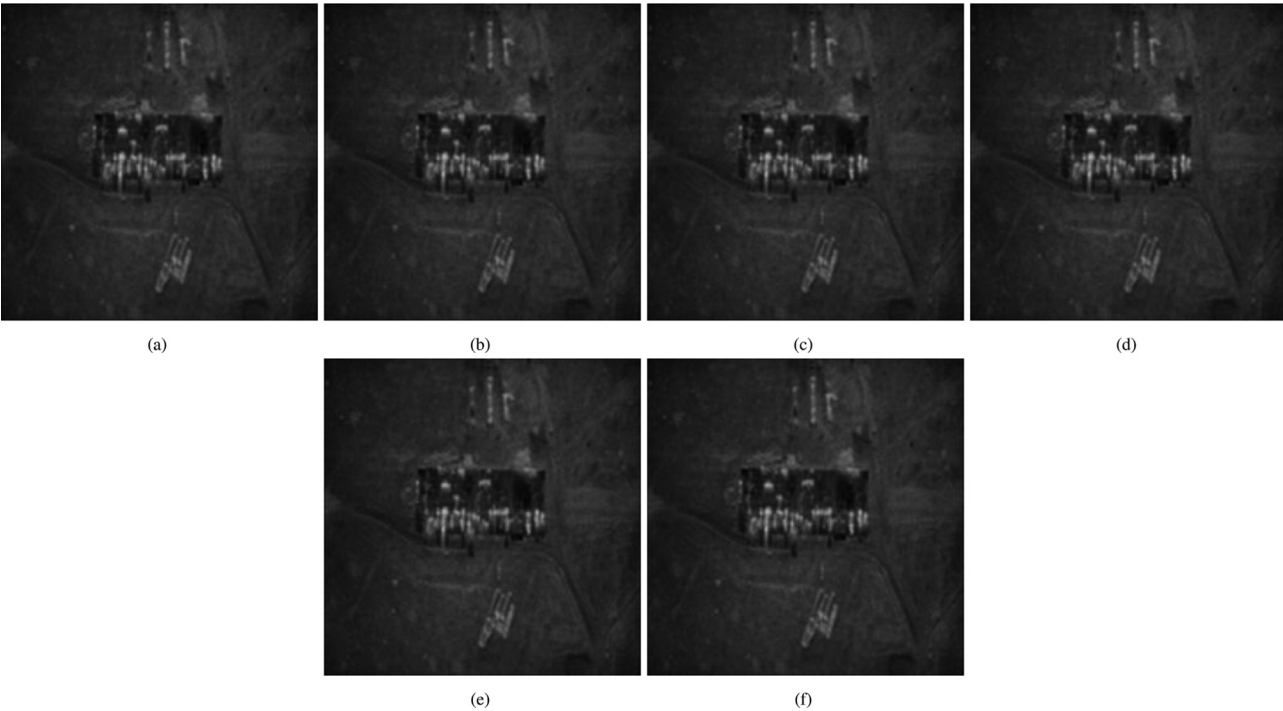


Fig. 7. Reconstructed SAR images using the SARBM3D filter for three different window sizes. (a)-(c) With speckle variance 0.01. (d)-(f) With Speckle variance 0.05.

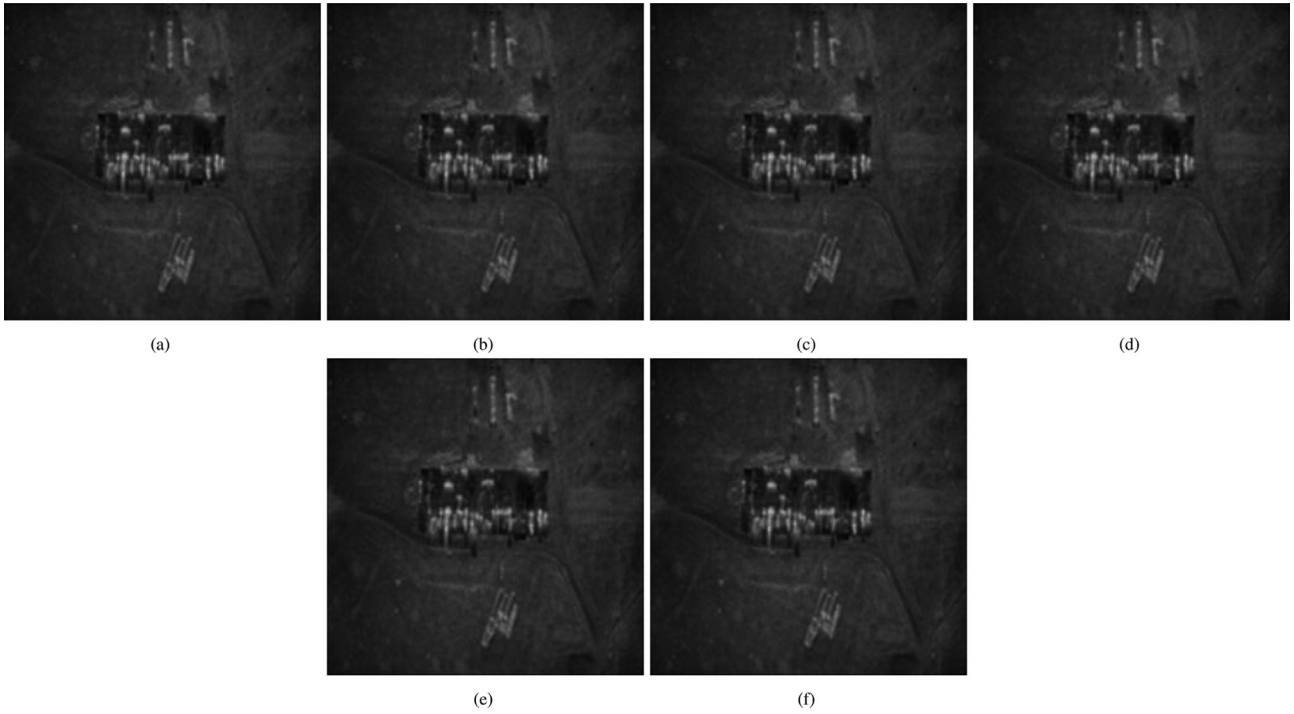


Fig. 8. Reconstructed SAR images using the Non-Local PCA-Based Filtering for three different window sizes. (a)-(c) With speckle variance 0.01. (d)-(f) With Speckle variance 0.05.

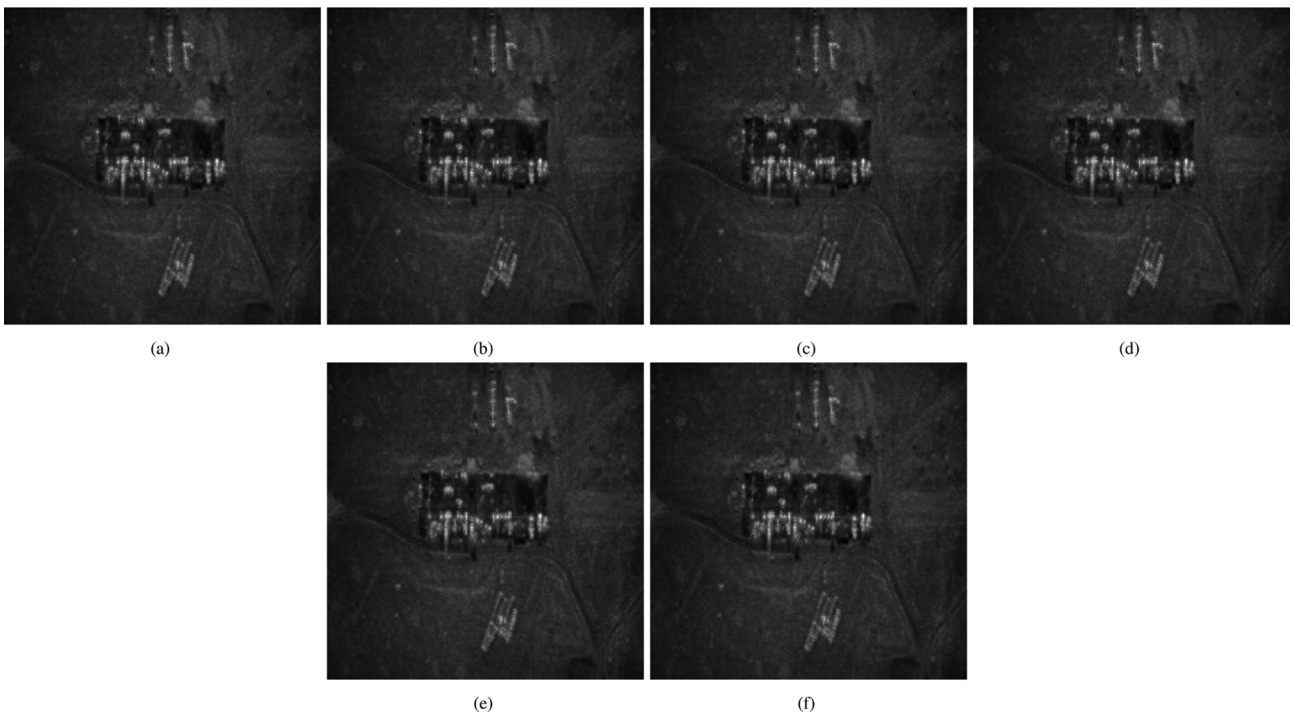


Fig. 9. Reconstructed SAR images using the IMMSE filter for three different window sizes. (a)-(c) With speckle variance 0.01. (d)-(f) With Speckle variance 0.05.

size 5x5 and 0.848 for a window size 7X7. These SSI values are compared with conventional filters. We observed that the SSI value is 0.841 is a lesser value for a window size 3X3. As shown in Table 2 the proposed filter SSIM parameter values are compared with conventional filters. The

SSIM value is 0.780 for a proposed filter with a window size of 3X3. This SSIM value is higher compared to conventional filters. Similarly, 0.570 is the SSIM value of the proposed filter having window size 3X3 which is a higher SSIM value compared to conventional filters as shown in

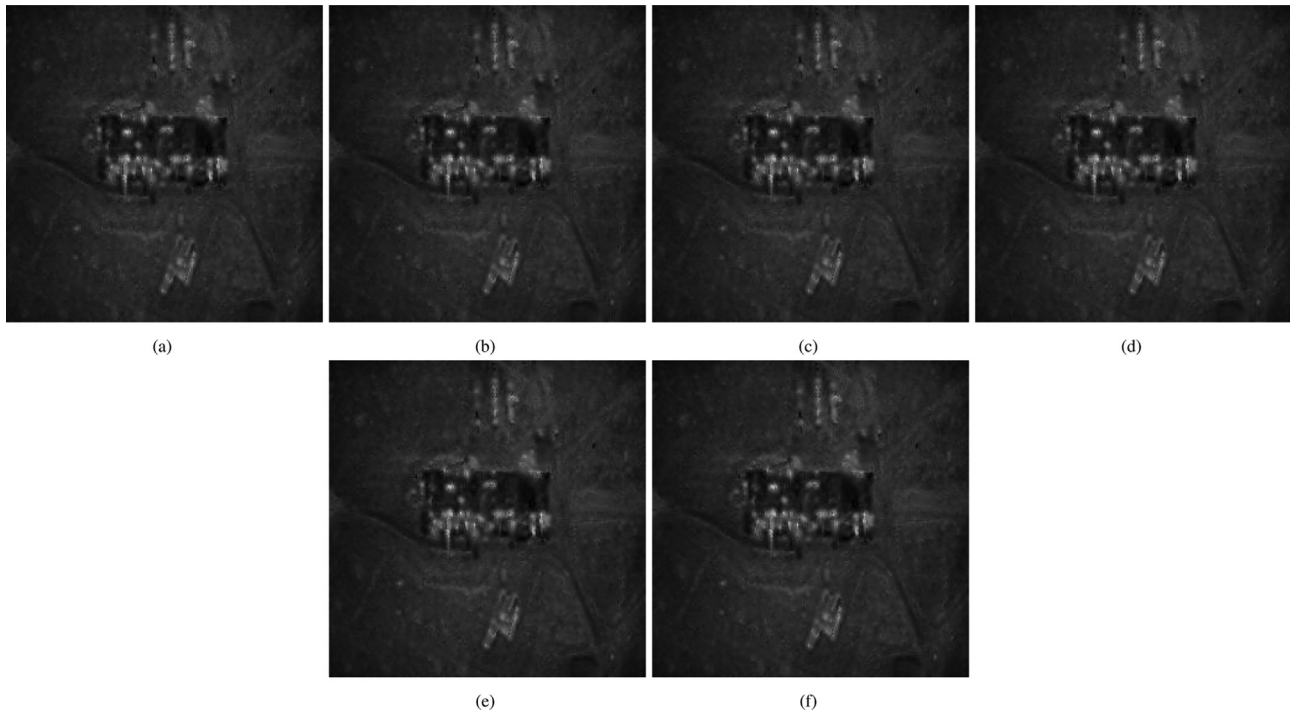


Fig. 10. Reconstructed SAR images using the Kirsch template filter for three different window sizes. (a)-(c) With speckle variance 0.01. (d)-(f) With speckle variance 0.05.

Table 1  
Comparison of SSI parameter for both proposed and conventional filleting methods.

Filtering methods	Speckle variance = 0.01			Speckle variance = 0.05		
	3X3	5X5	7X7	3X3	5X5	7X7
(Lee, 1980)	0.858	0.794	0.754	0.778	0.712	0.675
(Lopes et al., 1990)	0.869	0.815	0.785	0.790	0.731	0.703
(Kuan et al., 1985)	0.868	0.829	0.807	0.798	0.761	0.744
(Frost et al., 1982)	0.862	0.804	0.773	0.784	0.724	0.695
(Zhu et al., 2013)	0.877	0.803	0.759	0.803	0.728	0.685
SARBM3D	0.807	0.791	0.757	0.829	0.721	0.681
Non-Local PCA-Based Filter	0.821	0.805	0.769	0.835	0.749	0.699
IMMSE filter	0.881	0.839	0.829	0.863	0.769	0.759
Kirsch template filter	0.894	0.854	0.841	0.869	0.781	0.792
Proposed	0.648	0.652	0.645	0.632	0.636	0.624

Table 2  
Comparison of SSIM parameter for both proposed and conventional filleting methods.

Filtering methods	Speckle variance = 0.01			Speckle variance = 0.05		
	3X3	5X5	7X7	3X3	5X5	7X7
(Lee, 1980)	0.707	0.586	0.532	0.512	0.393	0.346
(Lopes et al., 1990)	0.701	0.580	0.526	0.511	0.390	0.344
(Kuan et al., 1985)	0.718	0.624	0.588	0.549	0.462	0.439
(Frost et al., 1982)	0.727	0.618	0.572	0.560	0.441	0.398
(Zhu et al., 2013)	0.704	0.589	0.535	0.506	0.391	0.343
SARBM3D	0.729	0.632	0.629	0.569	0.519	0.421
Non-Local PCA-Based Filter	0.731	0.645	0.746	0.572	0.522	0.435
IMMSE filter	0.778	0.785	0.789	0.596	0.563	0.536
Kirsch template filter	0.795	0.792	0.891	0.609	0.581	0.541
Proposed	0.780	0.650	0.590	0.570	0.490	0.450



Table 3

Comparison of ENL parameter for both proposed and conventional filtering methods.

Filtering methods	Speckle variance = 0.01			Speckle variance = 0.05		
	3X3	5X5	7X7	3X3	5X5	7X7
Speckled image	5.597	5.559	5.628	4.449	4.456	4.427
(Lee, 1980)	7.611	8.828	9.889	7.357	8.794	9.712
(Lopes et al., 1990)	7.410	8.373	9.122	7.122	8.339	8.971
(Kuan et al., 1985)	7.423	8.097	8.643	6.984	7.697	7.988
Frost (Frost et al., 1982)	7.537	8.589	9.426	7.218	8.512	9.168
(Zhu et al., 2013)	7.273	8.625	9.757	6.891	8.412	9.479
SARBM3D	7.562	8.012	8.931	7.441	7.134	7.926
Non-Local PCA-Based Filter	7.127	8.715	9.612	7.139	7.341	8.341
IMMSE filter	7.256	8.465	9.841	7.893	7.975	8.837
Kirsch template filter	7.652	8.561	9.527	8.249	7.983	8.931
Proposed	7.710	8.900	9.900	7.520	8.930	9.542

**Table 2.** The ENL value of a proposed filter is 7.71 which is a higher value compared to conventional filters as shown in Table 3. The proposed BEMD based adaptive Lee filter effectively removes the speckle noise near the edges. The Analysis of the proposed BEMD based filters has been carried out with various window sizes of 3X3, 5X5 and 7X7. Based on the analysis of the performance parameter values our proposed filter gives us better results. Finally, the proposed BEMD based adaptive Lee filter is more suitable for speckle noise reduction and details preservation.

## 6. Conclusion

In the present study, we have demonstrated the BEMD based adaptive Lee filtering approach for speckle noise minimization and accurate SAR image reconstruction. In the proposed filtering algorithm, three BIMF level decompositions are performed. We have used the first BIMF level input image to both adaptive filters and processed it. Different window sizes like 3X3, 5X5, and 7X7 have been used. The performance of the proposed filter algorithm is evaluated using various performance metrics, and the results are analyzed in detail to show the proof of the concept. The simulation results have shown good quality reconstruction in the SAR image, and the proposed filtering method able to suppress the speckle noise in the filtered image. The proposed filtering algorithm preserves more information in the SAR image compared to that of the other conventional methods. The work that has been done so far has the potential to be improved in the future through the development of optimal adaptive filters that are capable of being used in combination with multivariant decomposition methods.

## Declaration of Competing Interest

The authors declare that they have no known competing financial interests or personal relationships that could have appeared to influence the work reported in this paper.

## Acknowledgment

This research did not receive any specific grant from funding agencies in the public, commercial, or not-for-profit sectors

## References

- Baraldi, A., Parmiggiani, F., 1995. A refined gamma map sar speckle filter with improved geometrical adaptivity. *IEEE Trans. Geosci. Remote Sens.* 33 (5), 1245–1257.
- Bhuiyan, S.M., Attoh-Okine, N.O., Barner, K.E., et al., 2009. Bidimensional empirical mode decomposition using various interpolation techniques. *Adv. Adaptive Data Anal.* 1 (02), 309–338.
- Bhuiyan, S.M., Khan, J.F., Adhami, R.R., 2010. A novel approach of edge detection via a fast and adaptive bidimensional empirical mode decomposition method. *Adv. Adaptive Data Anal.* 2 (02), 171–192.
- Devapal, D., Kumar, S., Sethunadh, R., 2019. Discontinuity adaptive sar image despeckling using curvelet-based bm3d technique. *Int. J. Wavelets Multiresolut. Inf. Process.* 17 (03), 1950016.
- Dorini, L.B., Leite, N.J., 2013. A self-dual filtering toggle operator for speckle noise filtering. *Int. J. Image Graphics* 13 (03), 1350015.
- Elgamel, S., Soraghan, J., 2011. Empirical mode decomposition-based monopulse processor for enhanced radar tracking in the presence of high-power interference. *IET Radar, Sonar Navigat.* 5 (7), 769–779.
- Frost, V.S., Stiles, J.A., Shanmugan, K.S., et al., 1982. A model for radar images and its application to adaptive digital filtering of multiplicative noise. *IEEE Trans. Pattern Anal. Machine Intell.* 2, 157–166.
- Gao, Q., Zhang, D., Wang, Y., 2006. Speckle reduction in polarimetric sar imagery combining by pwf and stationary wavelet thresholding. *Int. J. Wavelets Multiresolut. Inf. Process.* 4 (04), 589–599.
- Jayanthi Sree, S., Vasanthanayaki, C., 2019. De-speckling of ultrasound images using local statistics-based trilateral filter. *J. Circ., Syst. Comput.* 28 (09), 1950150.
- Jian, Z., Zhao, B., Chen, Y., 2012. Application of bi-dimensional empirical mode decomposition (bemd) in extraction of platinum and palladium anomalies features. *Adv. Adaptive Data Anal.* 4 (01n02), 1250010.
- Jiang, C., He, X., 2017. An improved polsar image speckle reduction algorithm based on Immse and rica. *Mod. Phys. Lett. B* 31 (19–21), 1740033.
- Kabir, S.M., Bhuiyan, M.I.H., 2015. Modeling of log-transformed speckle noise in the contourlet transform domain for medical ultrasound images. *J. Circ., Syst. Comput.* 24 (02), 1540004.
- Kittisuwan, P., 2018. Speckle noise reduction of medical imaging via logistic density in redundant wavelet domain. *Int. J. Artif. Intell. Tools* 27 (02), 1850006.

- Kuan, D.T., Sawchuk, A.A., Strand, T.C., et al., 1985. Adaptive noise smoothing filter for images with signal-dependent noise. *IEEE Trans. Pattern Anal. Machine Intell.* 2, 165–177.
- Kumar, K.M., Velayudham, A., Kanthavel, R., 2017. An efficient method for road tracking from satellite images using hybrid multi-kernel partial least square analysis and particle filter. *J. Circ., Syst. Comput.* 26 (11), 1750181.
- Lee, J.-S., 1980. Digital image enhancement and noise filtering by use of local statistics. *IEEE Trans. Pattern Anal. Machine Intell.* 2, 165–168.
- Linderhed, A., 2009. Image empirical mode decomposition: A new tool for image processing. *Adv. Adaptive Data Anal.* 1 (02), 265–294.
- Liu, M., Wu, Y., Zhang, Q., et al., 2016. Synthetic aperture radar target configuration recognition using locality-preserving property and the gamma distribution. *IET Radar, Sonar Navigat.* 10 (2), 256–263.
- Lopes, A., Nezry, E., Touzi, R., et al., 1990. Maximum a posteriori speckle filtering and first order texture models in sar images. In: 10th annual international symposium on geoscience and remote sensing. Ieee, pp. 2409–2412.
- Lu, J., Chen, Y., Zou, Y., et al., 2017. A new total variation model for restoring blurred and speckle noisy images. *Int. J. Wavelets Multiresolut. Inf. Process.* 15 (02), 1750009.
- Mahdavi, S., Salehi, B., Moloney, C., et al., 2018. Speckle filtering of synthetic aperture radar images using filters with object-size-adapted windows. *Int. J. Digital Earth* 11 (7), 703–729.
- Myakinin, O.O., Kornilin, D.V., Bratchenko, I.A., et al., 2013. Noise reduction method for oct images based on empirical mode decomposition. *J. Innovat. Opt. Health Sci.* 6 (02), 1350009.
- Nunes, J.-C., Deléchelle, E., 2009. Empirical mode decomposition: Applications on signal and image processing. *Adv. Adaptive Data Anal.* 1 (01), 125–175.
- Passoni, L., Rabal, H., Arizmendi, C., 2004. Characterizing dynamic speckle time series with the hurst coefficient concept. *Fractals* 12 (03), 319–329.
- Sreelatha, P., Ezhilarasi, M., 2019. Improved adaptive wavelet thresholding for effective speckle noise reduction in low contrast medical images. *J. Circ., Syst. Comput.* 28 (10), 1950176.
- Sumaiya, M., Kumari, R.S.S., 2017. Comparative study of statistical modeling of wavelet coefficients for sar image despeckling. *Int. J. Wavelets Multiresolut. Inf. Process.* 15 (01), 1750003.
- Xu, L., Han, J., Wang, T., et al., 2019. Global image dehazing via frequency perception filtering. *J. Circ., Syst. Comput.* 28 (09), 1950142.
- Xu, Z.-H., Deng, Y.-K., Wang, R., 2016. Insights into prior learning for despeckling sar images. *IET Radar, Sonar Navigation* 10 (9), 1611–1618.
- Yang, D., Yu, C., Lv, L., et al., 2017. Sar image segmentation by selected principal components and kernel graph cuts ensembles. *Int. J. Pattern Recognit Artif Intell.* 31 (12), 1755015.
- Zhu, J., Wen, J., Zhang, Y., 2013. A new algorithm for sar image despeckling using an enhanced lee filter and median filter. In: 2013 6th International congress on image and signal processing (CISP), vol. 1, IEEE, pp. 224–228.